Tian *et al. BMC Neurology* (2025) 25:181
https://doi.org/10.1186/s12883-025-04166-9

BMC Neurology

RESEARCH Open Access

Analysis of the glymphatic system function in high-grade glioma patients using diffusion tensor imaging along perivascular spaces

Bin Tian[1], Xili Jiang[2], Xin Luo[1] and Wei Zhang[2*]

Abstract

Objectives This study seeks to determine if patients with high-grade glioma (HGG) demonstrate glymphatic system (GS) impairments using Diffusion Tensor Imaging Along Perivascular Spaces (DTI-ALPS). Additionally, it aims to examine the factors affecting GS performance and their implications for HGG prognosis.

Methods The study enrolled fifty HGG patients alongside fifty age- and sex-matched healthy individuals. Each participant underwent diffusion tensor imaging with a Philips 3.0T MRI scanner to assess and compute the ALPS index within perivascular spaces. Variables such as gender, grade, location, volume, peritumoral edema volume, mass-edema index (peritumoral edema volume/tumor volume) and ALPS index were recorded. The Student's t-test and rank sum test compared the ALPS indices between HGG patients and healthy controls to evaluate hemispheric differences. Linear and multivariate Cox regression analyses were utilized to discern factors influencing the ALPS index and to establish independent prognostic markers for HGG, respectively.

Results The ALPS indices in both hemispheres were significantly lower in HGG patients, with the ipsilateral hemisphere exhibiting further reduced levels than the contralateral ($P<0.001$). In comparisons involving tumor and edema volumes, no significant variations were observed between the hemispheres within HGG patients harboring larger tumors ($P=0.079$) or lesser edema volumes ($P=0.24$). A decrease in postoperative ALPS indices compared to preoperative figures was noted ($P<0.001$). Univariate linear regression indicated a negative relationship between the ipsilateral ALPS index and peritumoral edema volume ($P=0.0392$). Kaplan-Meier analysis demonstrated shorter survival times in patients with lower ALPS indices. Moreover, multivariate Cox regression highlighted tumor grade (HR = 1.548, $P=0.023$) and ipsilateral ALPS index (HR = 0.040, $P=0.003$) as crucial prognostic indicators.

Conclusion In patients with HGG, there is impaired GS function in both hemispheres of the brain. Additionally, the impaired GS function in the tumor-side hemisphere is associated with tumor-associated edema. Following surgery, further damage to GS function is observed in both hemispheres of the brain in HGG patients. Poor GS function in the tumor-side hemisphere is correlated with a worse prognosis in HGG patients.

Keywords Glymphatic system, MRI, High-grade glioma, DTI-ALPS, Perivascular spaces, Central nervous system

*Correspondence:
Wei Zhang
741793027@qq.com
[1]Department of Radiology, The Second People's Hospital of Hunan Province (Brain Hospital of Hunan Province), The School of Clinical Medicine, Hunan University of Chinese Medicine, Changsha 410021, China
[2]Department of Radiology, The Second People's Hospital of Hunan Province (Brain Hospital of Hunan Province), Changsha 410021, China

Introduction

In population-based research, glioma represents the predominant primary intracranial neoplasm. The World Health Organization (WHO) categorizes gliomas into four grades according to their histopathological features, with grades 3 and 4 designated as HGG. In HGG patients, disruption of the blood-brain barrier precipitates the development of peritumoral edemas and escalates intracranial pressure, substantially impairing the patients' life quality [1]. Continual increase in intracranial pressure may induce cerebral ischemia and subsequent edema, potentially leading to brain herniation, and mortality [2]. The median survival duration for HGG patients is approximately 15 months, and the five-year survival rate stands at a mere 5.6% [3]. The GS plays a vital role in expelling waste and maintaining fluid equilibrium within the brain parenchyma [4]. Cerebrospinal fluid (CSF), produced by the periventricular choroid plexus, permeates the brain parenchyma under the influence of aquaporin-4, mingling with the interstitial fluid (ISF) of the brain parenchyma, with the eventual discharge of ISF and its solutes through the perivascular spaces [5]. Monitoring changes in the GS among HGG patients is essential for elucidating glioma mechanisms and advancing treatment and prognostic strategies.

DTI-ALPS is an innocuous methodology for evaluating the GS's functionality through the dynamics of ISF in the human brain via diffusion MRI [6]. Research indicates a robust correlation between the ALPS index and traditional GS clearance evaluations conducted post-intrathecal gadolinium administration [7]. Moreover, a marked reduction in the ALPS index is observed in patients with normal pressure hydrocephalus, suggesting lymphoid impairment as confirmed by the protracted clearance after intrathecal gadobutrol administration [8, 9]. Consequently, the ALPS index functions as an effective surrogate indicator for detecting and quantifying deviations in lymphatic activity.

Although Toh and Zeng have discussed the impact of glioma characteristics on GS function, their findings regarding the effect of peritumoral edema on the ALPS index are contradictory. Furthermore, Zeng's study included gliomas of all grades in evaluating the prognostic value of GS function [10, 11]. Compared to low-grade gliomas (LGG), HGG exhibits more aggressive behavior and poorer prognosis. Therefore, investigating the relationship between GS function and HGG, while avoiding the potential misclassification of some LGG patients showing no difference in ALPS indices compared to healthy individuals, could provide further prognostic value. This study aims to explore the GS functional state in HGG patients and the impact of GS functional markers on the prognosis of HGG.

Materials and methods

Research target

This study initially enrolled 63 patients with pathologically confirmed high-grade glioma (HGG) from the Second People's Hospital of Hunan Province between 2018 and 2022. Based on predefined inclusion and exclusion criteria, 50 patients were ultimately included in the analysis. Thirteen patients were excluded for the following reasons: severe anatomical distortion caused by tumors ($n = 8$), motion artifacts ($n = 1$), and multicentric tumors involving bilateral cerebral hemispheres ($n = 4$). Additionally, fifty sex- and age-matched healthy subjects were enrolled as controls. All control participants had no history of neurological disorders or malignancies, demonstrated no abnormal findings on MRI (e.g., space-occupying lesions or white matter hyperintensities), and were excluded if they presented with subjective cognitive complaints, a history of head trauma, or cerebrovascular risk factors (e.g., hypertension, diabetes mellitus). The inclusion criteria were: (1) a diagnosis of HGG as per the 2021 fifth edition of the WHO Classification of Central Nervous System Tumors; (2) a tumor localized in either a unilateral cerebral hemisphere or one side of the posterior fossa (left or right), appropriate for DTI index assessment; (3) no prior treatment; (4) no significant white matter lesions; (5) no use of medications affecting the central nervous system. The exclusion criteria included: (1) the presence of other central nervous system organic lesions or psychiatric conditions; (2) prior receipt of adjuvant chemotherapy or radiotherapy; (3) tumor size or location that could compromise DTI index accuracy; (4) significant sleep disorders; (5) MRI contraindications.

Clinical and imaging information

Clinical and imaging data was collected, including gender, age, tumor volume, peritumoral edema volume, mass-edema index, and tumor location. Histopathological diagnosis was confirmed by a board-certified neuropathologist.

MRI

All MRI examinations were performed using a Philips Ingenia 3.0T superconducting MRI scanner equipped with a 16-channel head phased-array coil. The MRI protocol included pre- and post-contrast axial T1 and T2-weighted imaging, as well as axial fluid attenuation inversion recovery (FLAIR) sequences. Imaging parameters were: T1WI (TR = 2000ms, TE = 9ms), T2WI (TR = 6000ms, TE = 96ms), T2-FLAIR (TR = 6000 ms, TE = 85 ms). Specifications included a slice thickness of 5.0 mm, a slice gap of 1.0 mm, and a FOV of 245 mm × 245 mm. DTI scan settings featured: TR/TE = 9000/90 ms, a matrix of 128 × 128, a FOV of 200 × 200 mm, 64 diffusion gradient directions, a b-value of 1000, and a voxel

size of 2 mm × 2 mm × 2 mm with a slice thickness of 2 mm.

Image processing and analysis

Tumor and peritumoral edema boundaries were manually delineated slice-by-slice on imaging data by two radiologists using 3D Slicer 5.7.0. Regions of interest (ROI) that covered the entire area of tumor enhancement were manually outlined on the contrast-enhanced T1-weighted images. An additional ROI was defined on the T2-weighted FLAIR images to include both the peritumoral edema and the tumor. The volume of peritumoral edema was derived by subtracting the tumor-only ROI from the comprehensive ROI. In cases with multiple tumors, the aggregate volume of all lesions was calculated (Fig. 1).

The DTI-ALPS methodology was employed to assess glymphatic functionality by measuring diffusion rates along the perivascular spaces in the body of the lateral ventricle on a horizontal plane. DTI Studio software facilitated the measurement of DTI metrics. Using fractional anisotropy (FA) color maps at the level of the lateral ventricle body, fiber tracts and associated regions were identified. A 2 × 2 voxel cube ROI was positioned over these regions to capture diffusion rates on the X, Y, and Z axes, and these values were utilized to compute the DTI-ALPS index according to the prescribed formula:

$$\text{DTI} - \text{ALPS index} = \frac{\text{mean}(\text{Dxxproj}, \text{Dxxassoc})}{\text{mean}(\text{Dyyproj}, \text{Dzzassoc})}$$

In this model, Dxxproj and Dxxassoc are the diffusion coefficients for projection and associative fibers along the X-axis, respectively, while Dyyproj and Dzzassoc represent the diffusion coefficients for projection fibers along the Y-axis and associative fibers along the Z-axis, respectively.

Statistical analysis

Statistical analyses were performed using SPSS version 26.0. The Shapiro-Wilk and Levene tests determined the normality and homogeneity of variance for continuous variables. For data that were normally distributed and exhibited homogeneous variance, independent-sample t-tests were utilized to compare the two groups; alternatively, for skewed distributions or unequal variances, the Wilcoxon signed-rank test was implemented. Evaluations of ALPS indices across different categories considered factors such as tumor side (affected vs. contralateral hemisphere), tumor grade, tumor volume, peritumoral edema volume, and pre-operative vs. post-operative status, along with classifications based on tumor size. Patients were stratified into high and low groups based on the median tumor volume and peritumoral edema volume, respectively. Univariate linear regression analyzed correlations between ALPS indices and variables such as age, peritumoral edema volume, and mass-edema index in patients with HGG. Changes in bilateral ALPS indices before and after treatment in HGG patients were measured using Receiver Operating Characteristic (ROC) curves and the area under the curve (AUC). Kaplan-Meier curves were generated, and Log-rank tests were used to evaluate survival differences across groups. Cox regression analysis was applied to determine prognostic risk factors in HGG patients. Significance was set at a p-value of < 0.05.

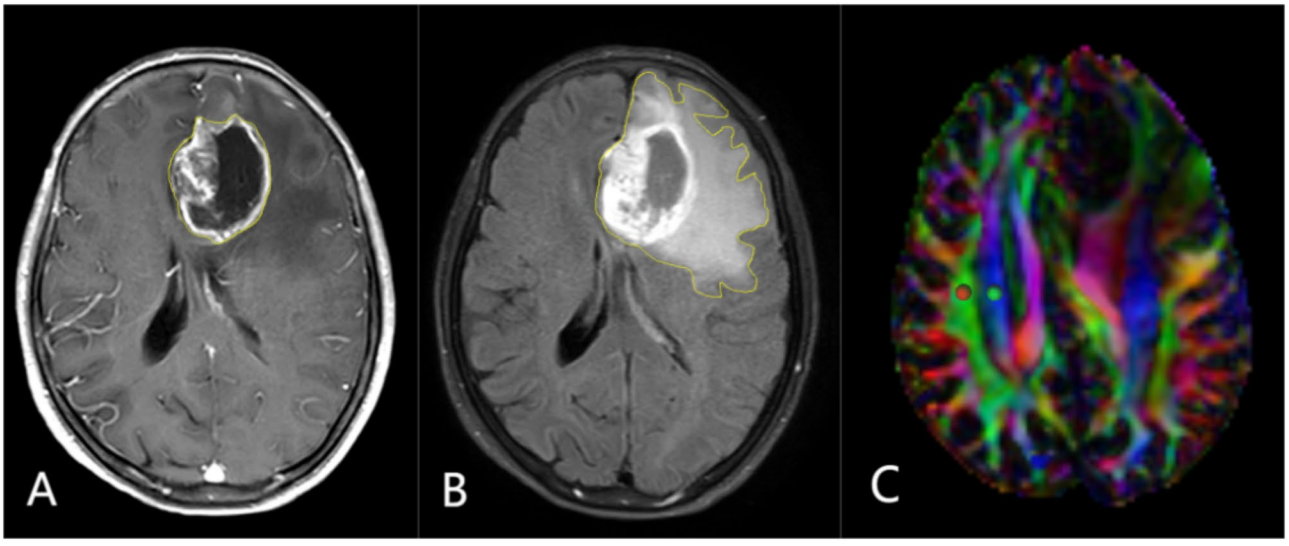

Fig. 1 Preoperative axial MRI slices of the brain in a patient. The contrast-enhanced T1-weighted sequence (**A**) shows tumor enhancement with central necrosis. The FLAIR sequence (**B**) reveals peritumoral edema. The directionally encoded color map (**C**) displays the ROI of the contralateral lateral ventricle perivascular regions, including projection fibers (green region) and association fibers (red region)

Table 1 Comparison of baseline data

parametric	HGG		Control group	statistical value	*P*-value
	left hemisphere	right hemisphere			
quantities	26	24	50		/
Age (years)	50.38 ± 14.88	50.42 ± 15.32	47.12 ± 13.39	0.670	0.514
Gender					
male	14	15	32	0.873	0.646
women	12	9	18		
Tumor grade					
3	9	9		0.045	0.832
4	17	15			
Tumor volume (mm^3)	42.25 (29.26, 70.98)	62.15 ± 39.16	/	-0.893	0.372
Edema volume (mm^3)	68.29 (45.17, 144.17)	86.88 ± 65.64	/	-0.680	0.497

Assessment of intra-observer and inter-observer variability for measuring peritumoral edema volume, tumor volume, and ALPS indices utilized the intraclass correlation coefficient (ICC) with 95% confidence intervals (CIs), following a two-way random-effects model. The definitive values for peritumoral edema volume, tumor volume, and ALPS indices were averages derived from two independent observers.

Results

This study included 50 HGG patients and 50 age- and sex-matched healthy controls. Among these patients, 26 had left-sided and 24 had right-sided HGG. Eighteen were assigned a Grade 3 classification, while thirty-two received a Grade 4 classification. There were no significant differences in age or sex between the two groups (Table 1).

ALPS indices were used as surrogate markers for glymphatic system function, respectively. The inter-observer consistency was good, with an ICC of 0.91 (95% CI).

As presented in Table 2, when comparing the bilateral ALPS indices of HGG patients with those of the age- and sex-matched control group, the indices of HGG patients were reduced ($P < 0.001$). Within the HGG cohort, the ALPS index was significantly lower on the tumor-affected side ($P < 0.001$). Further, the discrepancy in the ALPS index of the contralateral hemisphere between Grade 3 HGG patients and the control group was not significant ($P = 0.068$), and no notable differences were found in the bilateral ALPS indices in patients with either larger tumor volumes or smaller peritumoral edema volume ($P = 0.079$).

Figure 2 depicts the inter-group comparison results for the bilateral ALPS index among various tumor grades, tumor volumes, and peritumoral edema volume relative to the control group. Differences were noted in the contralateral hemisphere ALPS index between grade 3 and grade 4 gliomas, whereas the ipsilateral hemisphere ALPS index did not exhibit significant differences.

Figure 3 displays the outcomes of univariate linear regression analyses exploring factors influencing the bilateral hemisphere ALPS index within the HGG cohort. In this analysis, the ipsilateral hemisphere ALPS index demonstrated a negative correlation with peritumoral edema volume ($R^2 = 0.0856$, $P = 0.0392$), yet revealed no substantial correlations with age, tumor volume, or mass-edema index ($P > 0.05$). Furthermore, no linear correlations were found between the contralateral hemisphere ALPS index and age, tumor volume, peritumoral edema volume, or mass-edema index ($P > 0.05$). Figure 4

Table 2 Comparison between ALPS indices by different tumor grades, tumour location, tumour and oedema volume

parametric	Glioma group ($n = 50$)		Control group ($n = 50$)	#*P*-value	**P*-value	&*P*-value
	Ipsilateral ALPS index	Contralateral ALPS index				
Mean ALPS	1.36 ± 0.25	1.54 ± 0.19	1.73 ± 0.21	< 0.001	< 0.001	< 0.001
Tumor grade						
3	1.45 ± 0.26	1.62 ± 0.21		< 0.001	0.068	0.031
4	1.30 ± 0.23	1.50 ± 0.18		< 0.001	< 0.001	< 0.001
Tumor volume						
Large	1.38 ± 0.26	1.49 ± 0.18		< 0.001	< 0.001	0.079
Small	1.33 ± 0.25	1.59 ± 0.20		< 0.001	0.014	< 0.001
Edema volume						
Large	1.29 ± 0.25	1.52 ± 0.21		< 0.001	< 0.001	< 0.001
Small	1.42 ± 0.24	1.56 ± 0.19		< 0.001	0.001	0.24
Tumor location						
left hemisphere	1.35 ± 0.26	1.53 ± 0.21		< 0.001	< 0.001	0.004
right hemisphere	1.36 ± 0.24	1.55 ± 0.19		< 0.001	0.001	0.004

Note: # indicates comparison of ALPS index on the affected side of the glioma group with the control group; * indicates comparison of ALPS index on the contralateral side of the glioma group with the control group; & indicates comparison of ALPS index on the contralateral side of the glioma group with the affected side

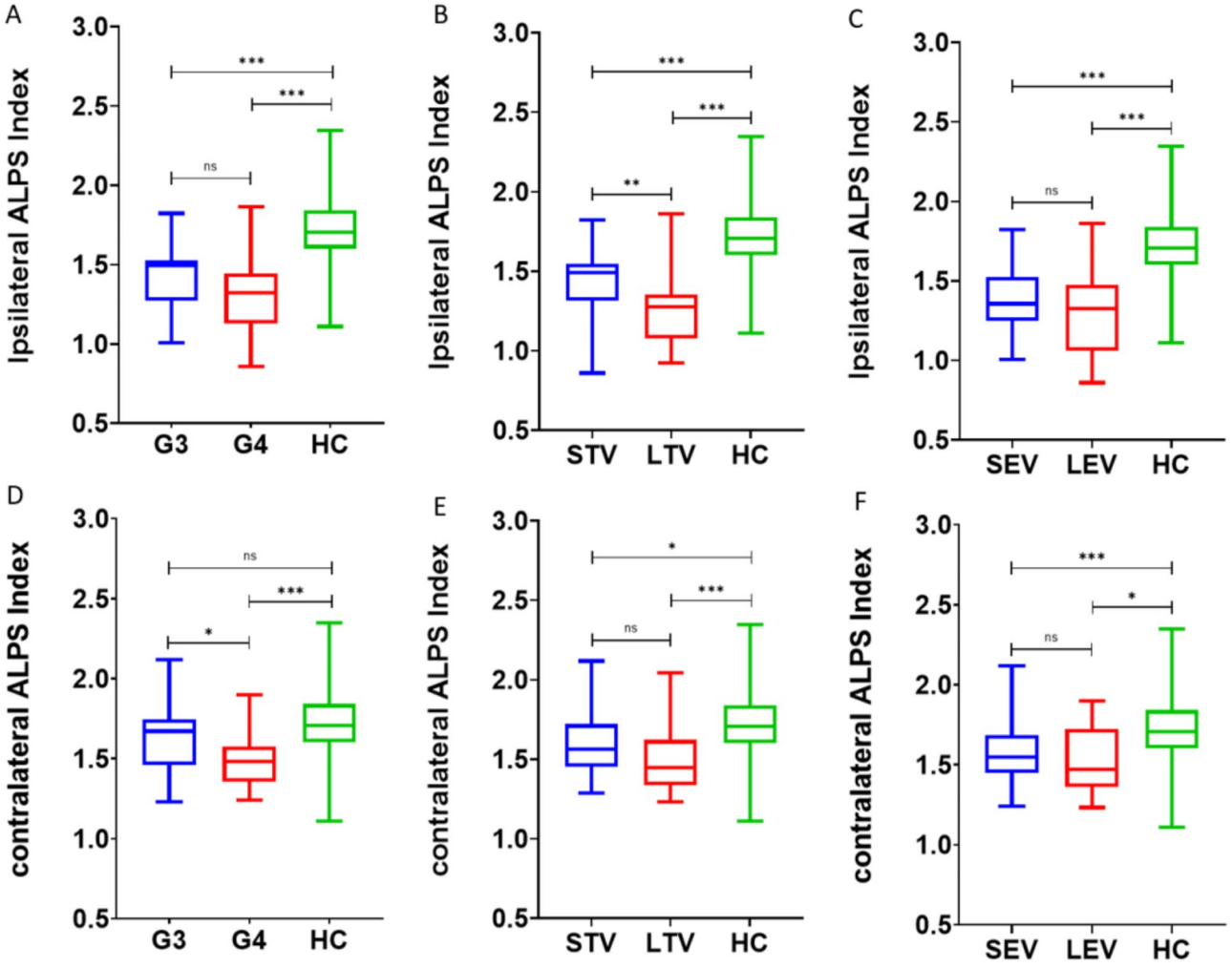

Fig. 2 Boxplot showing the differences in ipsilateral ALPS index with different tumor grades (**A**), tumor volume (**B**), and tumor edema volume (**C**), as well as the differences in contralateral ALPS index with tumor grading (**D**), volume (**E**), and edema volume (**F**). LTV, large tumor volume; LEV, large edema volume; STV, small tumor volume; SEV, small edema volume

demonstrates that the ALPS indices of both the ipsilateral and contralateral tumor sides were significantly lower in the postoperative group compared to the preoperative measurements, with statistically significant intergroup differences.

The ROC curve of the ipsilateral hemisphere ALPS index, which shows significant differences among HGG patients with different outcomes, was plotted to assess its prognostic value in HGG patients. The results indicate that the ipsilateral hemisphere ALPS index is an effective prognostic indicator for HGG patients (AUC = 0.7786, sensitivity = 66.67%, specificity = 84.38%) (Fig. 5A). Utilizing the optimal cutoff value from the ROC curve, HGG patients were segregated into low and high-value groups to evaluate their survival rates. As illustrated in Fig. 5B, Kaplan-Meier survival curves demonstrate that HGG patients with an ipsilateral hemisphere ALPS index ≥ 1.485 experienced longer overall survival (OS) (HR = 2.85, 95% CI 1.46–5.54, $P = 0.039$) (Fig. 5B). Table 3 summarizes a multivariate Cox analysis, indicating that tumor grade (HR = 1.548, 95% CI 1.166–2.057, $P = 0.023$) and ipsilateral hemisphere ALPS index (HR = 0.040, 95% CI 0.005–0.326, $P = 0.003$) are independent prognostic factors for HGG patients.

Discussion

This study confirmed that the ALPS indices in both hemispheres of HGG patients were significantly reduced compared to healthy controls, with the tumor-affected hemisphere showing a more pronounced decrease than the contralateral hemisphere. Such a significant disparity highlights more severe GS dysfunction in the tumor-affected hemisphere, consistent with previous studies on GS function in axial tumors [10]. Contrary to Toh et al. [11], who did not examine GS function in the contralateral hemisphere, our observations indicate no notable

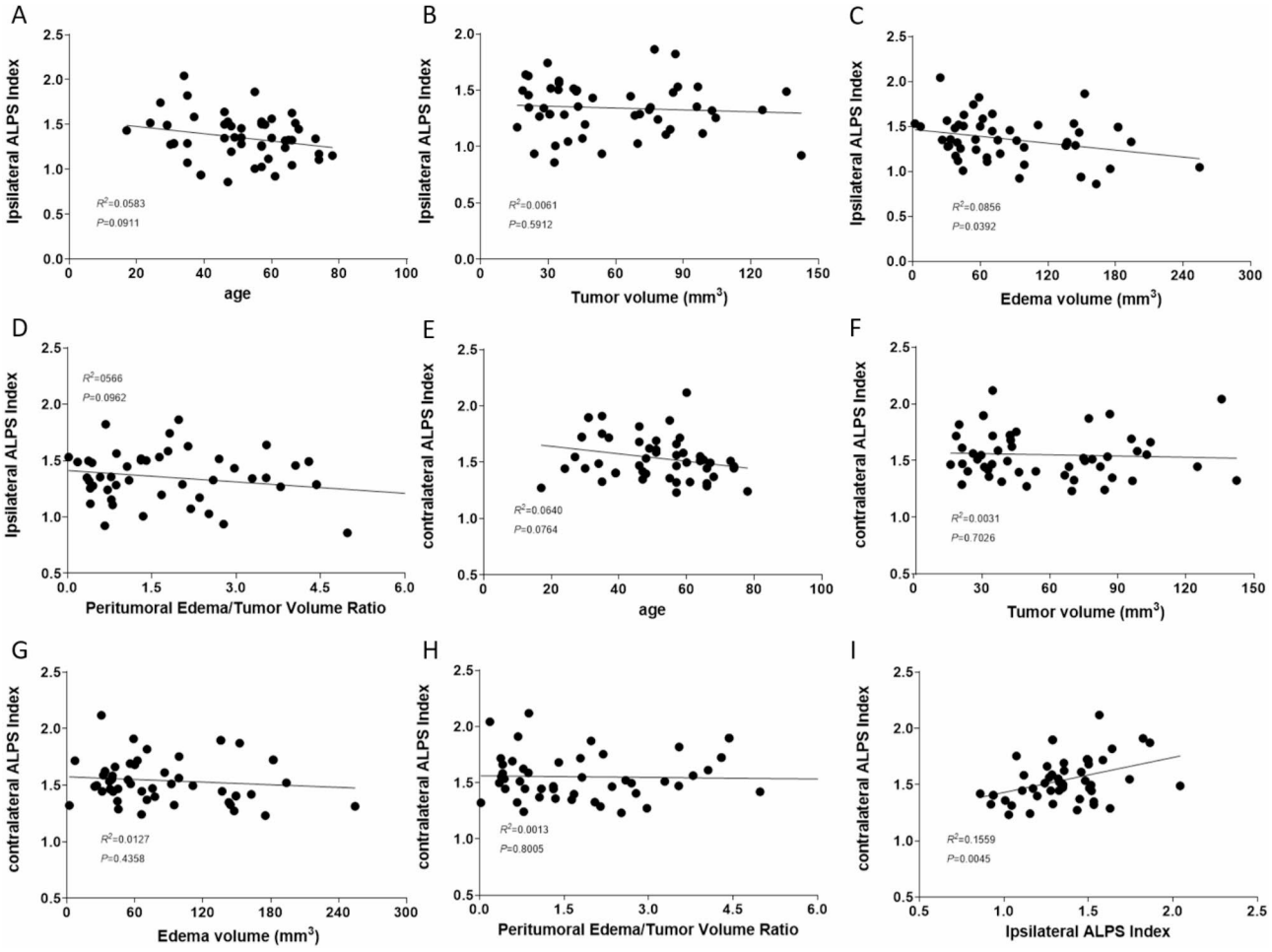

Fig. 3 Scatter plots with regression lines showing the correlation between age, tumor volume, tumor edema volume, and the ratio of tumor edema volume to tumor volume with ipsilateral ALPS index (**A-D**) and contralateral ALPS index (**E-H**). The scatter plot with a regression line (**I**) shows the correlation between ipsilateral and contralateral ALPS indices

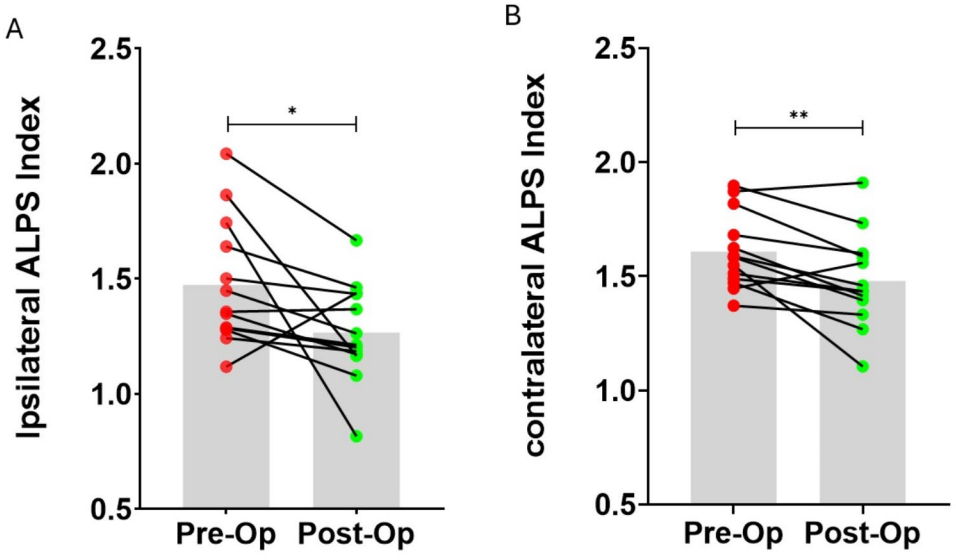

Fig. 4 Bar charts showing the preoperative and postoperative ALPS index differences in the ipsilateral (**A**) and contralateral (**B**) cerebral hemispheres of HGG patients who underwent surgical treatment

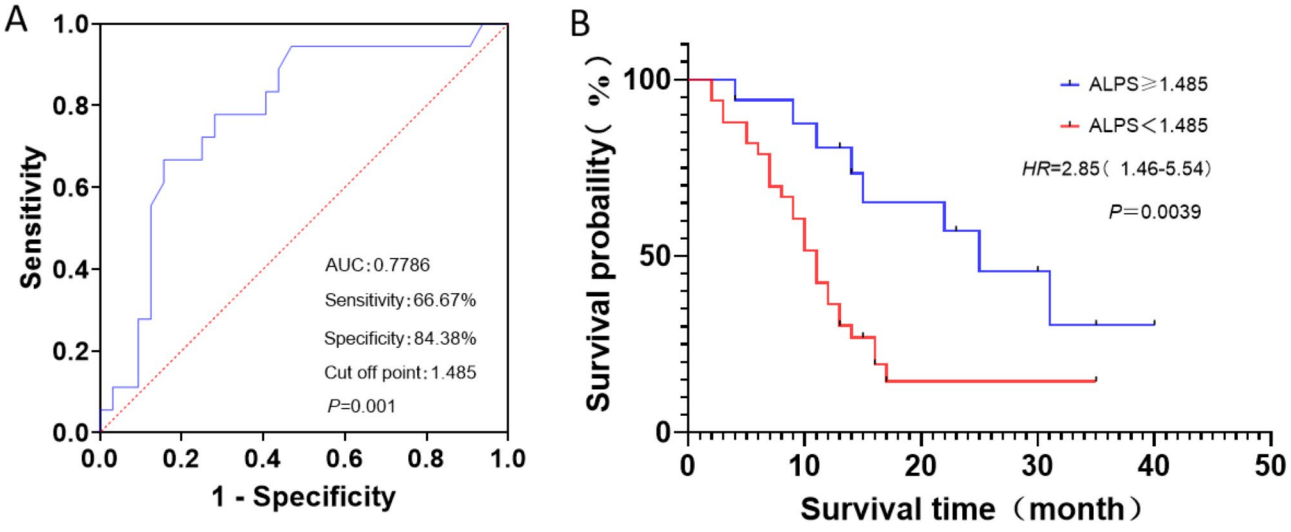

Fig. 5 ROC curve of the ipsilateral hemisphere ALPS index for prognosis in HGG patients (**A**) and Kaplan-Meier survival curve for different levels of ipsilateral ALPS index in the survival rate of HGG patients (**B**)

Table 3 Multivariate COX regression analysis

parametric	bias regression coefficient	*P*-value	Risk ratio (HR)	95.0% CI for HR	
				lower limit	limit
Gender	-0.511	0.208	0.600	0.271	1.329
Age (years)	0.012	0.427	1.012	0.983	1.041
Tumor grade	-2.054	0.023	1.548	1.166	2.057
Tumor volume	0.009	0.362	1.009	0.990	1.029
Edema volume	-0.013	0.061	0.987	0.974	1.001
mass-edema index	0.463	0.118	1.588	0.890	2.836
Contralateral ALPS index	-1.480	0.266	0.228	0.017	3.093
Ipsilateral ALPS index	-3.224	0.003	0.040	0.005	0.326

differences in the ipsilateral hemisphere ALPS index among various tumor grades, while variations were apparent in the contralateral hemisphere. The absence of variability in the ipsilateral hemisphere could be due to the robust proliferation and invasiveness of HGG [12–14], potentially obscuring differences in GS function impairment. Additionally, literature indicates possible asymmetry in GS dysfunction [15], significant radial asymmetry of white matter tracts [16], and differing degrees of GS function impairment in the contralateral hemisphere depending on tumor grade, explaining the variability in the contralateral hemisphere's ALPS index. Notably, the multicentric nature of high-grade gliomas may lead to small satellite lesions developing in the contralateral hemisphere that evade detection by conventional MRI due to their subclinical size. This phenomenon could mechanistically contribute to the observed differential ALPS index expression between tumor grades within the contralateral hemisphere. Our findings that the ALPS index in the contralateral hemisphere of grade 3 gliomas did not significantly differ from that in the healthy control group lend support to this hypothesis. Additionally, the smaller sample size for the tumor-side hemisphere ALPS calculation might have contributed to the observed discrepancies.

Currently, research suggests that GS dysfunction in brain tumors is the result of multiple internal factors. As the brain tumor volume increases, tumor compression of the perivascular spaces hinders CSF flow, leading to GS dysfunction [17]. In malignant brain tumors, in addition to mechanical tumor compression, cellular proliferation, angiogenesis, blood-brain barrier disruption, tumor infiltration, and inflammatory cell invasion are also significant factors contributing to GS dysfunction [18]. In this study, the ALPS index of the hemisphere adjacent to the tumor displayed a negative correlation with peritumoral edema volume, consistent with prior research on the tumor ALPS index [10, 11]. However, findings by Gao et al. [19] presented contrasting results; in their studies, this relationship was only significant in invasive meningiomas, with no notable correlations in malignant brain tumors. This variation could be linked to a compensatory upregulation of AQP4 in tumor-associated glial cells, which may diminish the link between GS dysfunction and elevated peritumoral edema volume [20, 21]. This suggests that the association between tumor-associated edema and GS dysfunction may still require further investigation.

Investigations into ALPS indices among healthy individuals and in conditions like Alzheimer's disease [22–27] showed a negative correlation with age, while studies in pediatric populations with autism spectrum disorder [28] and absence epilepsy [29] revealed a positive age

correlation. The negative age correlation commonly observed in adults older than 40 years might be attributed to a reduction in AQP4 channels in astrocytic end-feet and decreased CSF production due to lessened arterial pulsations [5, 30]. The positive correlation in younger cohorts likely reflects developmental progression. Our findings indicate no significant age-related correlation with the ALPS index in either hemisphere of tumor patients, aligning with results from diverse studies on brain tumors [11, 31], migraines [32], optic neuritis [33], and renal diseases [34], likely due to differing clinical conditions among participants.

The decrease in ALPS indices observed postoperatively in both hemispheres of HGG patients might result from the recent surgical interventions. While the reduction in the tumor-side hemisphere could arise from extensive tumor resection, other influences such as cranial and dura mater disruption impacting CSF dynamics, along with varying clinical treatments, medication, and sleep disturbances during hospitalization [35, 36], might also affect the ALPS index. Additionally, studies have indicated that the ALPS index in the contralateral hemisphere can exceed that of age-matched healthy controls [37], potentially due to compensatory GS dysfunction from the ipsilateral tumor. Therefore, ongoing postoperative follow-up in HGG patients is recommended for future studies.

GS, as a key mechanism in maintaining brain tissue fluid balance, also influences the tumor microenvironment. Radiotherapy, as a first-line treatment for gliomas, can regulate the tumor's immune microenvironment. Tumors with overexpressed vascular endothelial growth factor C (VEGF-C) in expanded meningeal lymphatic vessels are highly sensitive to radiotherapy, enhancing the efficacy of the treatment [38]. However, dysfunction of GS may impair the anti-tumor immune regulation triggered by radiotherapy. Therefore, GS function has a potentially evaluative value in glioma treatment and prognosis. In this research, the ALPS index of the ipsilateral hemisphere was correlated with the prognosis of HGG. Moreover, tumor-associated edema, a critical determinant of GS function, has been identified in previous studies as significant for evaluating and differentiating brain tumors through mass-edema index [39, 40], and for its prognostic relevance in brain metastases [41]. However, its examination in primary brain tumors remains infrequent. Our findings indicate that mass-edema index does not significantly correlate with the ALPS index, nor does it serve as a prognostic indicator for OS in HGG.

Although some studies use intrathecal gadolinium contrast MRI to more accurately assess brain lymphatic clearance function [42], this method is invasive and has several limitations, such as various indications and fixed intervals between MRI scans, making it difficult to widely apply clinically. DTI-ALPS, on the other hand, is a non-invasive, single-examination method with good inter-group consistency [6, 43] and it has been widely applied and validated in various central nervous system studies. This research has limitations, particularly that the ALPS index measures only the free diffusion within perivascular spaces along the x-axis and does not assess the total functionality of the brain's lymphatic system. Secondly, although most of the tumor data causing significant deformatiqon in the contralateral ventricle were excluded from this study, some deformation caused by tumors in the contralateral ventricle still could not be avoided, which may result in errors in the reflected indicators. It should be noted that the volumetric measurements of tumor and peritumoral edema using 3D Slicer software in this study were based on retrospectively collected 2D MRI sequences acquired with 5-mm slice thickness. This technical limitation may introduce measurement inaccuracies due to partial volume effects, particularly in quantifying small lesions at tissue interfaces. Lastly, the sample size of this study needs to be expanded, and further research should include continuous follow-up data to validate the changes between different features and indicators.

Conclusion

Our data suggest that reductions in the ALPS index among HGG patients signify GS dysfunction, especially on the tumor-side. The extent of GS dysfunction varies across different HGG grades and is more evident in the contralateral hemisphere. While the ipsilateral ALPS index inversely correlates with tumor-associated edema volume, further research is necessary to clarify the mechanisms linking tumor-associated edema with GS dysfunction. Moreover, the noted postoperative decrease in the ALPS index suggests a potential temporary reduction in GS functionality following surgical intervention. A lower ALPS index on the tumor-side independently correlates with an adverse prognosis in HGG patients.

Abbreviations

AUC	Area under the curve
CIs	Confidence Intervals
CSF	Cerebro spinal fluid
DTI-ALPS	Diffusion Tensor Imaging Along Perivascular Spaces
FA	Fractional Anisotropy
FLAIR	Fluid Attenuation Inversion Recovery
GS	Glymphatic system
HGG	High-grade glioma
ICC	Intraclass Correlation Coefficient
ISF	Iinterstitial fluid
LGG	Low-grade gliomas
LTV	Large tumor volume
LEV	Large edema volume
STV	Small tumor volume
SEV	Small edema volume
ROC	Receiver Operating Characteristic

ROI	Regions of interest
VEGF-C	Vascular Endothelial Growth Factor C
WHO	World Health Organization

Acknowledgements
We appreciated all the medical staff in our department of radiology and all colleagues in this study.

Author contributions
BT wrote the first draft of the manuscript and performed data collection. XJ conceived and designed the experiments. XL analyzed the data and prepared figures. WZ reviewed drafts of the paper and approved the final draft.

Funding
This work was supported by the Science Foundation of Hunan Health Commission (No. B202309017571).

Data availability
The data that support the findings of this study are available from the corresponding author upon reasonable request.

Declarations

Ethics approval and consent to participate
This study was approved by the Ethics Committee of The Second People's Hospital of Hunan Province (2022K031), and was conducted in accordance with the guidelines of the Declaration of Helsinki. Informed consent was obtained from the participants or their legal representatives.

Consent for publication
Not applicable.

Competing interests
The authors declare no competing interests.

Received: 3 February 2025 / Accepted: 28 March 2025
Published online: 25 April 2025

References

1. Das S, Marsden PA. Angiogenesis in glioblastoma. New Engl J Med. 2013;369(16):1561–3.
2. Fan JY, Kirkness C, Vicini P, Burr R, Mitchell P. Intracranial pressure waveform morphology and intracranial adaptive capacity. AM J Crit Care. 2008;17(6):545–54.
3. Ostrom QT, Gittleman H, Truitt G, Boscia A, Kruchko C, Barnholtz-Sloan JS. CBTRUS statistical report: primary brain and other central nervous system tumors diagnosed in the united States in 2011–2015. Neurooncology. 2018;20(suppl_4):iv1–86.
4. Rasmussen MK, Mestre H, Nedergaard M. The glymphatic pathway in neurological disorders. Lancet Neurol. 2018;17(11):1016–24.
5. Jessen NA, Munk ASF, Lundgaard I, Nedergaard M. The glymphatic system: A beginner's guide. Neurochem RES. 2015;40(12):2583–99.
6. Taoka T, Masutani Y, Kawai H, Nakane T, Matsuoka K, Yasuno F, Kishimoto T, Naganawa S. Evaluation of glymphatic system activity with the diffusion MR technique: diffusion tensor image analysis along the perivascular space (DTI-ALPS) in Alzheimer's disease cases. JPN J Radiol. 2017;35(4):172–8.
7. Zhang W, Zhou Y, Wang J, Gong X, Chen Z, Zhang X, Cai J, Chen S, Fang L, Sun J, et al. Glymphatic clearance function in patients with cerebral small vessel disease. NeuroImage. 2021;238:118257.
8. Eide PK, Ringstad G. Delayed clearance of cerebrospinal fluid tracer from entorhinal cortex in idiopathic normal pressure hydrocephalus: A glymphatic magnetic resonance imaging study. J Cerebr Blood F Met. 2019;39(7):1355–68.
9. Ringstad G, Vatnehol S, Eide PK. Glymphatic MRI in idiopathic normal pressure hydrocephalus. Brain. 2017;140(10):2691–705.
10. Zeng S, Huang Z, Zhou W, Ma H, Wu J, Zhao C, Yang Z, Qiu H, Chu J. Noninvasive evaluation of the glymphatic system in diffuse gliomas using diffusion tensor image analysis along the perivascular space. J Neurosurg 2024:1–10.
11. Toh CH, Siow TY. Factors associated with dysfunction of glymphatic system in patients with glioma. Front Oncol. 2021;11:744318.
12. Lan Y, Wang H, Chen A, Zhang J. Update on the current knowledge of lymphatic drainage system and its emerging roles in glioma management. Immunology. 2023;168(2):233–47.
13. Esemen Y, Awan M, Parwez R, Baig A, Rahman S, Masala I, Franchini S, Giakoumettis D. Molecular pathogenesis of glioblastoma in adults and future perspectives: A systematic review. Int J Mol Sci 2022, 23(5).
14. Sareen H, Ma Y, Becker TM, Roberts TL, de Souza P, Powter B. Molecular biomarkers in glioblastoma: A systematic review and Meta-Analysis. Int J Mol Sci 2022, 23(16).
15. Zhao X, Zhou Y, Li Y, Huang S, Zhu H, Zhou Z, Zhu S, Zhu W. The asymmetry of glymphatic system dysfunction in patients with Temporal lobe epilepsy: A DTI-ALPS study. J Neuroradiol. 2023;50(6):562–7.
16. Wright AM, Wu Y, Chen N, Wen Q. Exploring radial asymmetry in MR diffusion tensor imaging and its impact on the interpretation of glymphatic mechanisms. J Magn Reson Imaging 2023.
17. Toh C, Castillo M, Wong AM, Wei K, Wong H, Ng S, Wan Y. Differentiation between classic and atypical meningiomas with use of diffusion tensor imaging. AM J Neuroradiol. 2008;29(9):1630–5.
18. Preusser M, Haberler C, Hainfellner JA. Malignant glioma: neuropathology and neurobiology. Wien Med Wochenschr. 2006;156(11–12):332–7.
19. Gao M, Liu Z, Zang H, Wu X, Yan Y, Lin H, Yuan J, Liu T, Zhou Y, Liu J. A histopathologic correlation study evaluating glymphatic function in brain tumors by multiparametric MRI. Clin Cancer Res. 2024;30(21):4876–86.
20. Lin Z. Glioma-related edema: new insight into molecular mechanisms and their clinical implications. Chin J Cancer. 2013;32(1):49–52.
21. Gomolka RS, Hablitz LM, Mestre H, Giannetto M, Du T, Hauglund NL, Xie L, Peng W, Martinez PM, Nedergaard M et al. Loss of aquaporin-4 results in glymphatic system dysfunction via brain-wide interstitial fluid stagnation. Elife 2023, 12.
22. Hsu J, Wei Y, Toh CH, Hsiao I, Lin K, Yen T, Liao M, Ro L. Magnetic resonance images implicate that glymphatic alterations mediate cognitive dysfunction in alzheimer disease. Ann Neurol. 2023;93(1):164–74.
23. Cai X, Chen Z, He C, Zhang P, Nie K, Qiu Y, Wang L, Wang L, Jing P, Zhang Y. Diffusion along perivascular spaces provides evidence interlinking compromised glymphatic function with aging in Parkinson's disease. CNS Neurosci Ther. 2023;29(1):111–21.
24. Hsiao W, Chang H, Hsu S, Lee C, Huang S, Cheng C, Huang C, Chang C. Association of cognition and brain reserve in aging and glymphatic function using diffusion tensor Image-along the perivascular space (DTI-ALPS). Neuroscience. 2023;524:11–20.
25. Wang J, Zhou Y, Zhang K, Ran W, Zhu X, Zhong W, Chen Y, Li J, Sun J, Lou M. Glymphatic function plays a protective role in ageing-related cognitive decline. Age Ageing 2023, 52(7).
26. Lee DA, Lee J, Park KM. Glymphatic system impairment in patients with status epilepticus. Neuroradiology. 2022;64(12):2335–42.
27. Lee DA, Park BS, Ko J, Park SH, Park J, Kim IH, Lee YJ, Park KM. Glymphatic system function in patients with newly diagnosed focal epilepsy. Brain Behav. 2022;12(3):e2504.
28. Li X, Ruan C, Zibrila AI, Musa M, Wu Y, Zhang Z, Liu H, Salimeen M. Children with autism spectrum disorder present glymphatic system dysfunction evidenced by diffusion tensor imaging along the perivascular space. Medicine. 2022;101(48):e32061.
29. Pu W, Wei S, Qiu M, Chen X, Zou W, Ge Y, Qiu W. Dysfunction of the glymphatic system in childhood absence epilepsy. Front Neurosci-Switz. 2023;17:1312676.
30. Kress BT, Iliff JJ, Xia M, Wang M, Wei HS, Zeppenfeld D, Xie L, Kang H, Xu Q, Liew JA, et al. Impairment of paravascular clearance pathways in the aging brain. Ann Neurol. 2014;76(6):845–61.
31. Toh CH, Siow TY, Castillo M. Peritumoral brain edema in metastases May be related to glymphatic dysfunction. Front Oncol. 2021;11:725354.
32. Lee DA, Lee H, Park KM. Normal glymphatic system function in patients with migraine: A pilot study. Headache. 2022;62(6):718–25.
33. Cacciaguerra L, Carotenuto A, Pagani E, Mistri D, Radaelli M, Martinelli V, Filippi M, Rocca MA. Magnetic resonance imaging evaluation of perivascular space abnormalities in neuromyelitis Optica. Ann Neurol. 2022;92(2):173–83.
34. Heo CM, Lee DA, Park KM, Lee YJ, Park S, Kim YW, Ko J, Yoo BC, Park BS. Glymphatic system dysfunction in patients with early chronic kidney disease. Front Neurol. 2022;13:976089.
35. Iliff JJ, Wang M, Liao Y, Plogg BA, Peng W, Gundersen GA, Benveniste H, Vates GE, Deane R, Goldman SA, et al. A paravascular pathway facilitates CSF flow

through the brain parenchyma and the clearance of interstitial solutes, including amyloid beta. Sci Transl Med. 2012;4(147):147ra111.
36. Xie L, Kang H, Xu Q, Chen MJ, Liao Y, Thiyagarajan M, O'Donnell J, Christensen DJ, Nicholson C, Iliff JJ, et al. Sleep drives metabolite clearance from the adult brain. Science. 2013;342(6156):373–7.
37. Villacis G, Schmidt A, Rudolf JC, Schwenke H, Kuchler J, Schramm P, Ulloa P. Evaluating the glymphatic system via magnetic resonance diffusion tensor imaging along the perivascular spaces in brain tumor patients. JPN J Radiol. 2024;42(10):1146–56.
38. Zhou C, Ma L, Xu H, Huo Y, Luo J. Meningeal lymphatics regulate radiotherapy efficacy through modulating anti-tumor immunity. Cell Res. 2022;32(6):543–54.
39. Baris MM, Celik AO, Gezer NS, Ada E. Role of mass effect, tumor volume and peritumoral edema volume in the differential diagnosis of primary brain tumor and metastasis. Clin Neurol Neurosur. 2016;148:67–71.
40. Reyes Soto G, Vega-Moreno DA, Catillo-Rangel C, Gonzalez-Aguilar A, Chavez-Martinez OA, Nikolenko V, Nurmukhametov R, Rosario Rosario A, Garcia-Gonzalez U, Arellano-Mata A, et al. Correlation of edema/tumor index with histopathological outcomes according to the WHO classification of cranial tumors. Cureus J Med Sci. 2024;16(11):e72942.
41. Chow KKH, Meola A, SD Chang. Commentary: peritumoral edema/tumor volume ratio: A strong survival predictor for posterior fossa metastases. Neurosurgery. 2019;85(1):E18–9.
42. Yamamoto EA, Bagley JH, Geltzeiler M, Sanusi OR, Dogan A, Liu JJ, Piantino J. The perivascular space is a conduit for cerebrospinal fluid flow in humans: A proof-of-principle report. P Natl Acad Sci USA. 2024;121(42):e1887721175.
43. Taoka T, Ito R, Nakamichi R, Kamagata K, Sakai M, Kawai H, Nakane T, Abe T, Ichikawa K, Kikuta J, et al. Reproducibility of diffusion tensor image analysis along the perivascular space (DTI-ALPS) for evaluating interstitial fluid diffusivity and glymphatic function: changes in alps index on multiple condition acquisition eXperiment (CHAMONIX) study. JPN J Radiol. 2022;40(2):147–58.

Publisher's note